Inorg. Chem. **1992**, *31*, 727–731 727

Articles

Contribution from the Departamento de Química, Universidad de Cantabria, 39005-Santander, Spain,
and Instituto de Catálisis y Petroleoquímica, CSIC, Madrid, Spain

Synthesis and Characterization of Al–Ga Pillared Clays with High Thermal and Hydrothermal Stability

F. González,[*,†] C. Pesquera,[†] C. Blanco,[†] I. Benito,[†] and S. Mendioroz[‡]

Received June 27, 1991

This work describes the preparation and characterization of a new PILC material with mixed pillars of Al^{3+} and Ga^{3+} intercalated between the layers of montmorillonite. Various Al/Ga ratios are studied in order to obtain the most suitable physicochemical properties and the maximum stability of the products. The basal spacing of the samples obtained varies between 18.7 and 19.9 Å at room temperature and between 17.5 and 17.7 Å after thermal treatment at 500 °C. The resulting material has a high thermal stability, maintaining 71% of its specific surface area after being heated at 700 °C for 2 h under a dry air current. Its hydrothermal stability is also optimal: it retains 100% of its specific surface after treatment for 2 h at 500 °C under a current of air saturated with water vapor at 40 °C. Moreover, the surface of this material presents a large number of acid centers.

Introduction

Pillared clays are a new family of materials obtained by using inorganic polyoxycations to form pillars between the layers of smectitic silicates. With a suitable choice of polyoxycations the separation between layers can be kept stable. The resulting material has a high specific surface and a characteristic porous structure which is of great interest because of its potential application in various fields.[1]

One of the fields of application is catalysis.[2] Pillared smectites have acid properties which make them suitable for use in petrochemical cracking where they can successfully replace zeolites. An advantage that pillared clays have with respect to zeolites is that the diameter of their micropores is greater, which allows larger molecules, and therefore heavier oil fractions, to be cracked. However, a difficulty involved in using these materials is that they are disactivated by the coke deposited during cracking and must be treated with water vapor at high temperatures to regenerate them. The pillared laminar silicates, PLS, obtained until now,[3] including those pillared with polyoxycations of Al, which have been studied most, do not have sufficient stability and collapse at temperatures below 500 °C, with a loss of interlaminar space, surface area, and activity.

In order to avoid the sintering of the layers of clay, the thermal resistance of the pillars must be increased. One of the ways of achieving this end which has been tried by a number of authors[4–7] is the introduction of mixed pillars. Given the similarity of the chemical properties of these clays and zeolites, we thought of trying to achieve this end by using Ga^{3+} as a stabilizing cation in the pillars of Al polyoxycations, in analogy with experiments carried out with zeolites.[8,9]

Although PILCs with only the Ga polyoxycation had been investigated,[10,11] mixed Al–Ga pillaring had not been studied. When the first brief communications[12] of our results along these lines was in press, a closely related article reporting the preparation and stability of GaAl–PILC in comparison with Ga–PILC and Al–PILC was published.[13] The purpose of our present work is to study the conditions under which the Ga^{3+} cation can stabilize the structure of an Al–PILC and to analyze the effects of this mixed pillaring on the thermal and hydrothermal stability of this material. The evolution with temperature of the micro- and mesoporosity is also presented, along with the acid properties of the products that were obtained.

Experimental Section

A. Starting Material. The clay used as the raw material is a bentonite from *Serrata de Níjar* (Almeria, Spain), supplied by Minas de Gador SA. Its structural formula, which was determined previously,[14] is as follows:

$$Si_{8.00}(Al_{2.69}Fe_{0.32}Mg_{0.97})O_{20}(OH)_4(Ca_{0.13}Mg_{0.26}Na_{0.23}K_{0.02})$$

It was purified by fractionated sedimentation with the fraction $<2\ \mu m$ being collected. Homoionic montmorillonite was obtained by means of cation exchange using a 1 M solution of NaCl. Next, it was washed until the Cl^- ion was eliminated. The sample obtained in this way, which will be denoted by Mont-Na, had a surface area of 87 m^2/g and a pore volume of 0.084 cm^3/g, at $P/P_0 = 0.98$. Its exchange capacity was 59 mequiv/100 g of clay, and its basal spacing was 15.4 Å, which decreased to 9.9 Å at 500 °C.

B. Equipment and Methods. The following equipment and techniques were used for the physicochemical characterization of the materials:

Chemical analysis was carried out by atomic absorption spectrometry with a Perkin-Elmer 560 instrument.

X-ray diffraction diagrams were determined on the powder with the particles oriented so as to increase the intensity of the 001 reflection using a Philips PW-1710 diffractometer with Cu Kα radiation.

SEM and energy-dispersive X-ray analysis (EDXRA) were carried out with a Jeol electron microscope (Model JSM-T 330 A) with a Link Analytical AN 10.000 microanalyzer.

Thermal analysis was performed in a Setaram TG-DSC 111 apparatus, with a N_2 flow of 20 cm^3/min and a heating rate of 5 °C/min.

Thermal and Hydrothermal Treatment. The samples were subjected to temperatures of 500 and 700 °C for 2 h in a fixed-bed reactor. In the thermal treatment, a current of 100 cm^3/min of dry air was used, while

---

[†] Universidad de Cantabria.
[‡] Instituto de Catálisis y Petroleoquímica.

(1) Mitchell, I. V. *Pillared layered structures, current trends and applications*; Elsevier Applied Science: London, 1990.
(2) Barrault, J.; Zivkev, C.; Bergaya, F.; Gatineau, L.; Hassoun, N.; Van Damme, H.; Mari, D. *J. Chem. Soc., Chem. Commun.* **1988**, 1403.
(3) Burch, R. *Pillared Clays. Catalysis Today*; Elsevier: New York, 1988; Vols. 2 and 3.
(4) Carrado, K. A.; Suib, S. L.; Skoularikis, N. D.; Coughlin, R. W. *Inorg. Chem.* **1986**, *25*, 4217.
(5) Occelli, M. L. *J. Mol. Catal.* **1986**, *35*, 377.
(6) Lee, W. L.; Tatarchuk, J. *Hyperfine Interact.* **1988**, *41*, 661.
(7) Sterte, J. *Clays Clay Miner.* **1991**, *39*, 167.
(8) Mandreck, G. P.; Smith, T. D. *J. Chem. Soc., Faraday Trans. 1* **1989**, *85* (10), 3215.
(9) Bradley, S. M.; Kydd, R. A.; Yamdagni, J. *J. Chem. Soc., Dalton Trans* **1990**, *2*, 413.
(10) Bellaloui, A.; Plee, D.; Meriaudeau, P. *Appl. Catal.* **1990**, *63*, L7.
(11) Vieira, A.; Poncelet, G. *Pillared layered structures, current trends and applications*; Mitchell, I. V., Ed.; Elsevier Applied Science: London, 1990; p 185.
(12) González, F.; Pesquera, C.; Benito, I.; Mendioroz, S. *J. Chem. Soc., Chem. Commun.* **1991**, 587.
(13) Bradley, S. M.; Kydd, R. A. *Catal. Lett.* **1991**, *8*, 185.
(14) Pesquera, C. Thesis, University of Oviedo, 1989.

0020-1669/92/1331-0727$03.00/0 © 1992 American Chemical Society

Table I. Variables in the Synthesis of the Samples

sample	% Al	pH of olig	pH of clay + olig begining	 end	Al^{3+}, mequiv/g	Ga^{3+} mequiv/g	% Al incorp	g of Ga/100 g of clay
A	100	4.02			9.7		100	0
B	75	3.36	3.58	5.26	1.6	3.9	29.6	9.3
C	50	3.30	3.44	4.63	1.2	8.5	12.6	16.2
D	25	2.84	3.08	4.49	0.2	13.1	1.7	28.2
E	0	2.44	2.64	4.34		12.1	0	23.9

in the hydrothermal treatment the same volume of air was used but it was saturated with water vapor by means of a bubbler at 40 °C.

IR Spectroscopy Acidity Study. Infrared spectra were obtained with a single-beam Perkin-Elmer Model 1605 FT-IR spectrophotometer, with a sensitivity of ±4 cm^{-1} in the 1700–1400-cm^{-1} range and ±1% in transmittance. Self-supporting wafers were prepared by pressing ca. 25 mg of sample on a 18-mm-diameter die. The wafer was degassed by heating at 200 °C for 2 h in vacuo before performing pyridine adsorption on the sample for 30 min. Infrared spectra were recorded after evacuation at room temperature and also after evacuation was carried out for 2 h at various temperatures from 100 to 400 °C.

Determination of Textural Parameters. Specific surface was determined by adsorption of N_2 at 77 K in a Micromeritics ASAP 2000 instrument and then by application of the BET equation to the first points of the isotherm.[15]

Meso- and microporosity were studied by analyzing the N_2 adsorption isotherms up to relative pressures close to 1. The total *Vp* was considered to be the volume of N_2 liquid adsorbed at a relative pressure of 0.98. Microporosity was determined by the MP method of Brunauer,[16] applied to the adsorption data for relative pressures less than 0.3. Mesoporosity was analyzed by the BJH method.[17]

Synthesis. Preparation of the Pillaring Agent. The Al–Ga polyoxycations were prepared by starting with 0.2 M solutions of $AlCl_3 \cdot 6H_2O$ + $GaCl_3$, with different Al/Ga ratios (see Table I), and gradually adding appropriate volumes of 0.5 M NaOH solution to obtain a OH/(Al + Ga) ratio of 2.0. Then, the reaction mixture was diluted with the quantity of water necessary to yield an (Al^{3+} + Ga^{3+}) concentration of 0.1 M. The solutions obtained in this way were aged at 60 °C for 2 h.

Pillaring Process. The solutions of pillaring agent with different Al/Ga ratios (Table I) were added with vigorous stirring to a clay slurry of 2.5 g/100 mL with pH 7.24 which had been kept in water for 15 days to ensure maximum swelling of the sheets. The final proportion in all cases was 20 mequiv of (Al + Ga)/g of clay, with a solid/liquid ratio of 0.5%. The reaction mixture was stirred continuously for 24 h at room temperature. Then, it was washed by means of dialysis with distilled water using 1 L/g of clay. Dialysis was continued with the water being renewed every 24 h until Cl^- ion concentrations decreased to the point where the conductivity of the wash water was <30 μS. Finally, it was centrifuged and dried in an oven at 60 °C.

Table I shows the different variables in the preparation of the five samples obtained in this way. The column corresponding to each sample indicates the following data: denomination of the sample; percentages of Al/Ga used in the preparation of the oligomer; pH of the oligomer after aging; pH of the clay + oligomer solution at the beginning and end of dialysis; amount of cation incorporated into the pillared product, expressed as mequiv of Al^{3+}/g of clay and mequiv of Ga^{3+}/g of clay. The data on the quantity of these cations incorporated were determined by means of chemical analysis of Al^{3+} and Ga^{3+} in the liquid remaining after centrifuging and washing the mixture which resulted from the pillaring process. In the case of Ga, data were also determined directly by means of EDXRA on the solid, expressed as grams of Ga/100 g of clay.

Characterization. X-ray Diffraction. Figure 1 compares the evolution of the X-ray diffractograms between 3 and 12° (2ϑ) of the samples subjected to thermal treatment at 500 °C as well as the untreated ones. Considering first the untreated samples, it can be seen that sample A, which is pillared only with Al, displays a *d*(001) peak at 18.9 Å. With the progressive incorporation of Ga, this peak is gradually displaced up to 19.8 Å. In all the diagrams except that of sample A, there is a broad peak between 10.6 and 11.5 Å, whose intensity increases with the Ga content. This second peak suggests that as the proportion of Ga is increased the fraction of clay that remains unpillared becomes greater. This could indicate that the amount of oligomer available for pillaring becomes insufficient as the proportion of Al diminishes or the competition of Ga may hinder the diffusion of the oligomer between the sheets of montmorillonite. In comparison with the initial Al/Ga proportions, the incorporation of Al into the pillared product does indeed decrease sharply with respect to that of Ga (Table I).

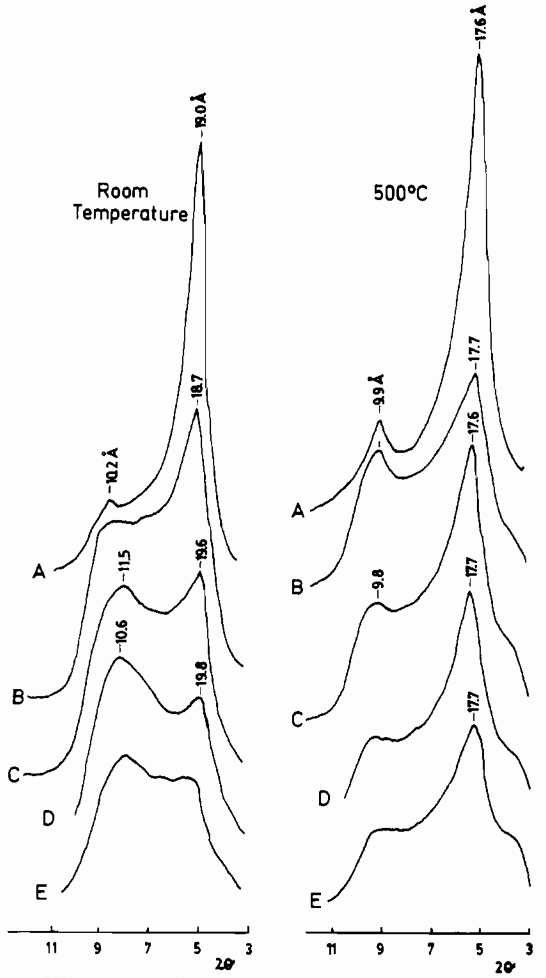

Figure 1. XRD plots of the samples: (a) room temperature; (b) 500 °C.

In the samples treated at 500 °C, the basal spacing is reduced slightly, with the values of the *d*(001) peak being at 17.7 Å. The symmetry and intensity of this peak increase, confirming the existence of pillared material that is stable up to this temperature. The second peak is displaced to 9.9 Å, which corresponds to the basal spacing of sodium montmorillonite with sintered sheets. This confirms the existence of part of the material in an unpillared form. It can be deduced that the height of the pillars is between 7.5 and 8.3 Å by subtracting the thickness of the mineral sheet from the basal spacing.

Thermal Analysis. Figure 2 shows the thermograms of samples A–D. The thermograms of Mont-Na, i.e. the initial sample of sodium montmorillonite, display two steps, one up to 200 °C, which corresponds to the loss of surface-adsorbed water (7.02%), and another one at 600 °C, corresponding to the dehydroxylation of the silicate structure (5.61%). In the successive samples, a peak appears in the DTG between 200 and 415 °C. The intensity of this peak increases as the amount of Ga incorporated into the material becomes greater. At the same time, the intensity of the peak between 350 and 730 °C decreases and a shoulder appears at 600 °C, which becomes progressively more intense.

The following comments can be made about the variations observed with respect to the initial sample. The loss of surface-adsorbed water is proportional to the specific surface of the different samples, as will be

---

(15) Gregg, S. J.; Sing, K. S. W. *Adsorption Surface Area and Porosity*; Academic Press: London, 1982.

(16) Brunnauer, S.; Skalny, J.; Odler, J. Pore Structure and Properties of Minerals. In *Proceedings of the International Symposium at Rilem*; IUPAC: Prague, 1973; p 1–26.

(17) Barrett, E. P.; Joyner, L. G.; Halenda, P. P. *J. Am. Chem. Soc.* **1951**, *73*, 373.

Table II. Textural Parameters of the Samples at Room Temperature and at 700 °C

	S_{BET}, m^2/g		V_{ad}, cm^3/g		V_{microp}, cm^3/g		V_{acum}, cm^3/g	
sample	25 °C	700 °C	25 °C	700 °C	25 °C	700 °C	25 °C	700 °C
A	384	115	0.216	0.155	0.119	0.018	0.078	0.163
B	288	204	0.206	0.192	0.083	0.050	0.131	0.142
C	227	161	0.179	0.169	0.066	0.040	0.116	0.135
D	136	65	0.154	0.148	0.036	0.008	0.133	0.150
E	107	45	0.156	0.160	0.025	0.003	0.147	0.171

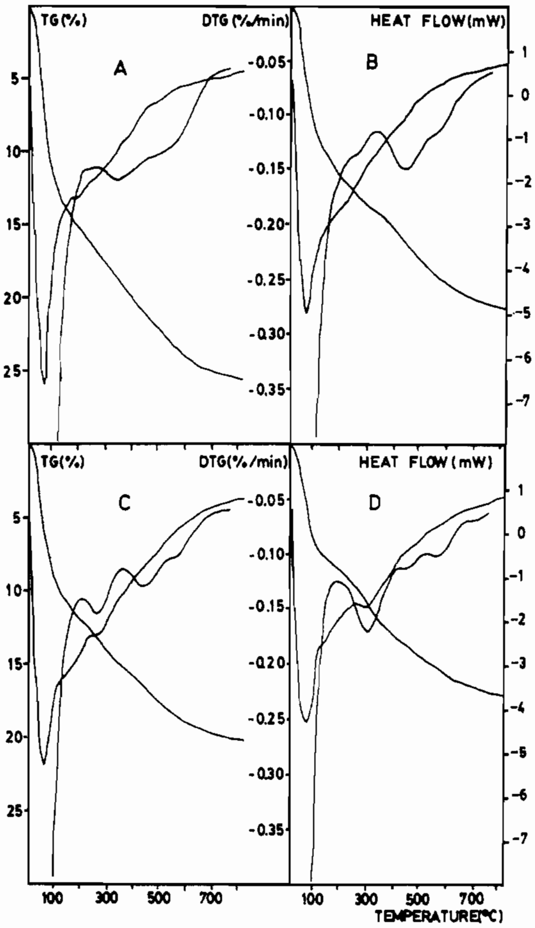

Figure 2. Thermograms of the samples.

seen later. The new peak that appears between 200 and 415 °C in the samples with Ga could be attributed to the dehydration of the Ga^{3+} cations. The peak between 350 and 730 °C is attributable to the water of the pillars, and the shoulder at 600 °C to the dehydroxylation of the fraction of montmorillonite that remains unpillared, which increases with the amount of Ga incorporated, as was pointed out in the preceding section.

N_2 Adsorption–Desorption Isotherms. Figure 3 shows the isotherms of N_2 at 77 K corresponding to samples A–E and those for samples A-500, A-700, B-500, and B-700, which were selected from the samples treated thermally for the purpose of comparison. In the zone of low values of p/p_0, Langmuir type I adsorption isotherms are observed, which indicates the presence of micropores; in the zone of high values of p/p_0, they are type IV, corresponding to mesoporous solids.[7] The hysteresis loop is type H3, attributable to adsorbents having slit-shaped pores between parallel layers. This type of loop is distorted in the isotherm of sample E, which has 100% Ga, with the desorption curve displaying a gradual decline from $p/p_0 = 1$. The curve of sample D represents an intermediate case between that of sample E and the others. In the samples of material B that were treated thermally, it can be seen that the types of isotherms and hysteresis loops are maintained. However, a widening of the hysteresis loop is observed with the increase in temperature, which can be attributed to greater delamination, with the concomitant increase in adsorption of N_2 between parallel layers.

Table II presents the values of S_{BET}, V_{ads} at $p/p_0 = 0.98$, V_{microp} and V_{acum} of the different samples at room temperature and at 700 °C. Analyzing the distribution of mesopores (values of V_{acum} up to a pore diameter of 20 Å in Table II and the distribution in Figure 4), we can distinguish two zones: pores larger than 50 Å and those smaller than this diameter. The percentage of these smaller pores diminishes as we go from sample A to E. This means that as the amount of Ga in the samples increases, the pore distribution shifts toward larger diameters.

The hydrothermal stability of the surface and pillars was studied by means of the N_2 isotherms of the samples subjected to hydrothermal treatment. The results, which are compiled in Table III, allow us to compare the values of S_{BET}, V_{microp}, V_{acum}, and V_{ads} at $p/p_0 = 0.98$ for the samples treated at 500 °C, with and without water vapor.

Electron Microscopy. The photographs shown in Figure 5 illustrate the differences in the morphology of samples A–D. As the percentage

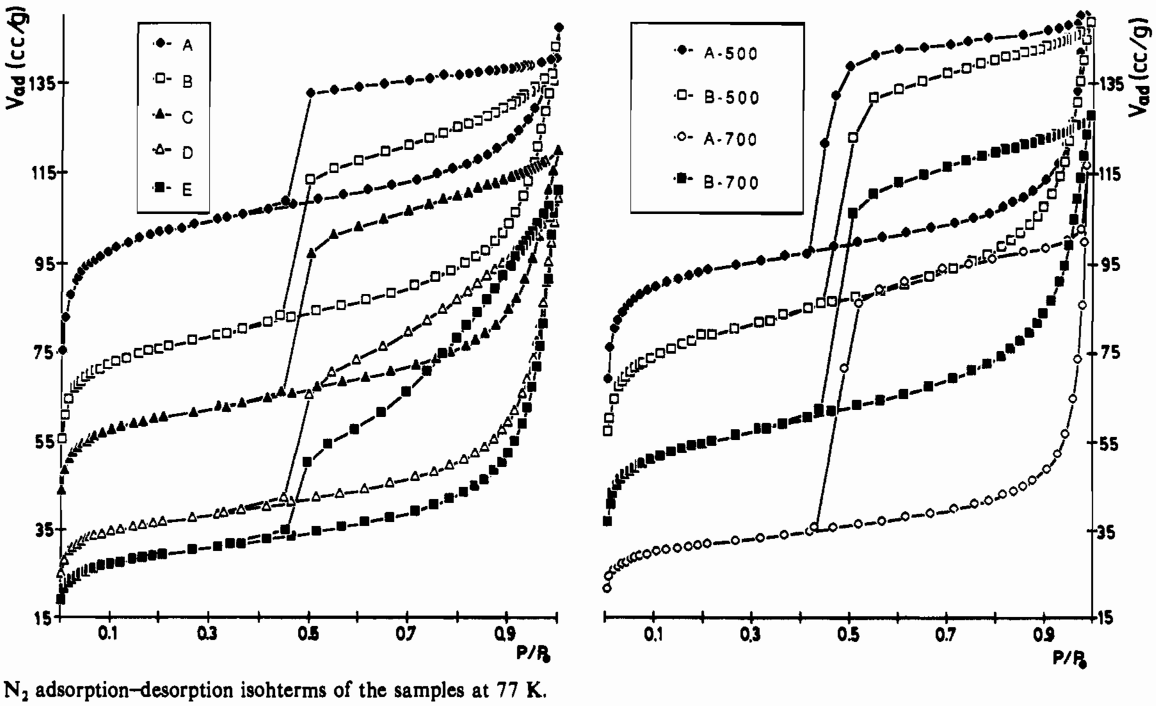

Figure 3. N_2 adsorption–desorption isohterms of the samples at 77 K.

Table III. Textural Parameters of the Samples Treated at 500 °C under Air Current with and without Water Vapor

	S_{BET}, m²/g		V_{ad}, cm³/g		V_{microp}, cm³/g		V_{acum}, cm³/g	
sample	with	without	with	without	with	without	with	without
A	76	353	0.125	0.252	0.013	0.111	0.172	0.173
B	295	287	0.215	0.217	0.080	0.079	0.140	0.139
C	235	232	0.198	0.194	0.064	0.069	0.135	0.133

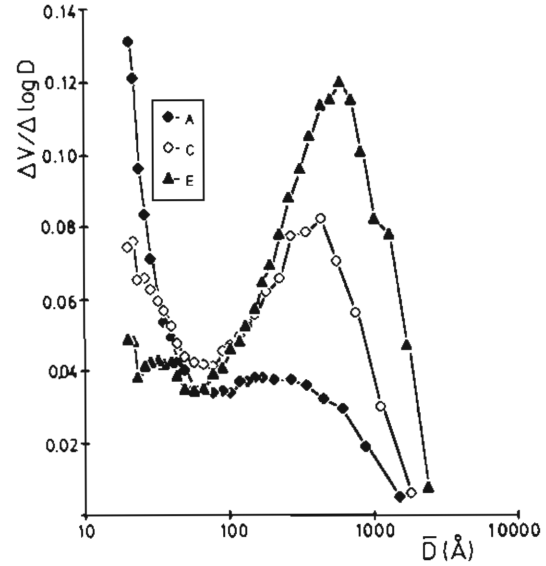

Figure 4. Mesopore distribution of the different samples.

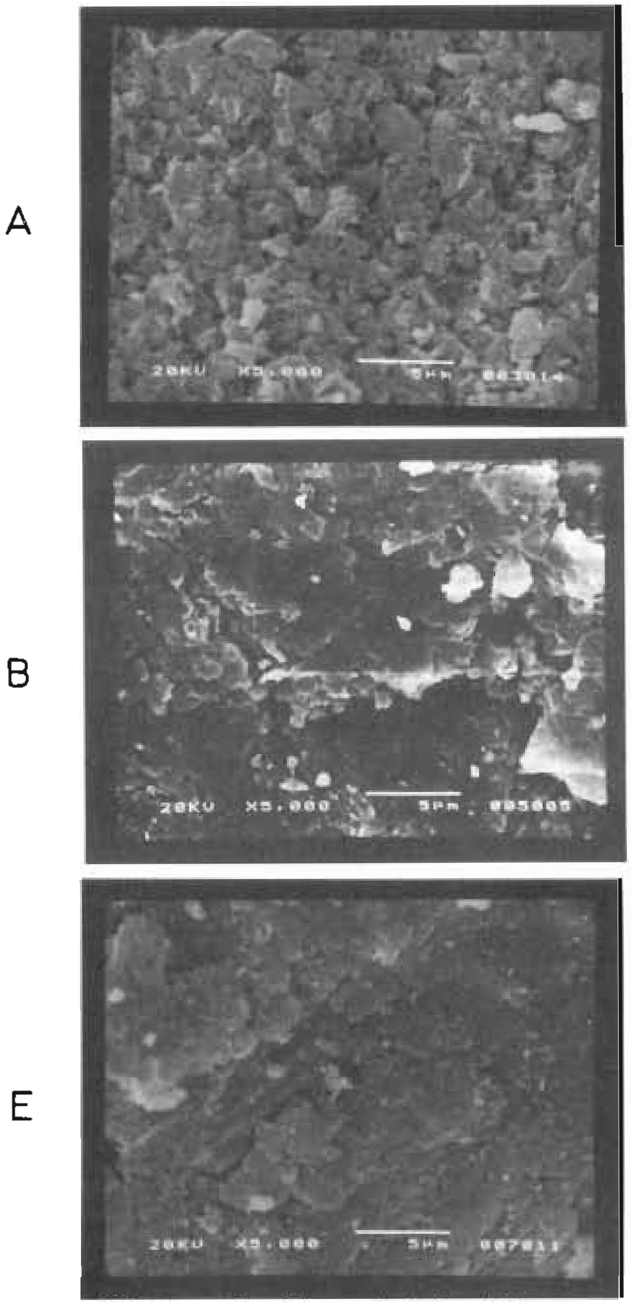

Figure 5. SEM micrographs of the samples A, B, and E.

of Ga increases, the samples become progressively more covered with a wrinkled coat which prevents us from observing clearly the exfoliation characteristic of the material pillared with Al. The analysis with EDX-RA (energy-dispersive X-ray analysis) indicates that the content of Ga rises from sample B to E (Table I) and that the Ga is homogeneously distributed at all points of the material considered.

Study of the Acidity of the Samples by IR Spectroscopy. Figure 6 shows the infrared spectra in the region 1700–1400 cm^{-1} of pyridine adsorbed on sodium homoionic montmorillonite after degassing in vacuo at different temperatures. The sample treated at 200 °C after pyridine adsorption exhibits the bands at 1445 and 1601 cm^{-1} and a shoulder at 1600 cm^{-1}, which are assigned to Lewis centers, and a band at 1489 cm^{-1}, attributed to both Lewis and Brönsted acid sites.[18] There is also a small band at 1546 cm^{-1} and a shoulder at 1638 cm^{-1} due to Brönsted acid sites. The unusual Brönsted acidity in this sample may be due to exchangeable cations that were not exchanged when the homoionic sample was prepared, as Figueras[19] has pointed out. Subsequent to degassing at 400 °C, only pyridine coordinated to Lewis acid sites is detected.

Figure 6 also shows the IR spectrum of pyridine adsorbed on montmorillonite pillared with Al (sample A). The spectrum of this sample recorded after pyridine adsorption and heating for 2 h at 200 °C shows the bands of the spectrum of the sodium montmorillonite, but they are more intense. The spectrum at 200 °C shows that the intensity of the adsorption band at 1445 cm^{-1}, which is due to pyridine chemisorbed on Lewis acid sites, is far stronger than that of the band at 1546 cm^{-1}, due to pyridine adsorbed on Brönsted acid sites. At 400 °C, the band associated to pyridine coordinated to Lewis acid sites is intense, and shoulders at 1554 and 1638 cm^{-1} due to Brönsted sites are detected. The intensities of bands assigned to Lewis centers appear to be almost temperature independent in the 100–400 °C range.

The spectrum of sample B (Figure 6) shows few differences with respect to sample A. The intensities of bands assigned to pyridine coordinated on Lewis acid sites up to 200 °C are weaker and wider in this sample than in sample A, probably because there is an overlap of two different types of Lewis acid sites due to Al and Ga in the pillars and also because the number of mequiv of Al + Ga/g of clay (Table I) is smaller in this sample than in sample A. These two samples show a parallel behavior in the evolution of the bands with thermal treatment.

Discussion

In the X-ray diffractograms of Figure 1 it can be appreciated by observing the intensity of the peaks that as we go from sample A to E the percentage of material involved in pillaring becomes smaller. The total number of mequiv of Al^{3+} + Ga^{3+} incorporated into the solid material (Table I) decreases in sample B and then increases in the following samples, with the Ga^{3+} content rising while that of Al^{3+} is falling. For both cations, the percentages of material incorporated are far below the corresponding theoretical compositions of the starting reactants. These experimental data together with the peak that appears in the thermograms between 200 and 450 °C lead us to believe that not all the Ga^{3+} cations incorporated take part in pillar formation but instead a fraction of them are found as exchange cations of the silicate. The SEM micrographs also reflect the incorporation of material onto the surfaces of the layers, which display a wrinkled appearance with the material deposited obscuring the characteristic laminar

---

(18) Parry, E. R. *J. Catal.* **1963**, *2*, 371.
(19) Figueras, F. *Catal. Rev. Sci. Eng.* **1988**, *30*, 457.

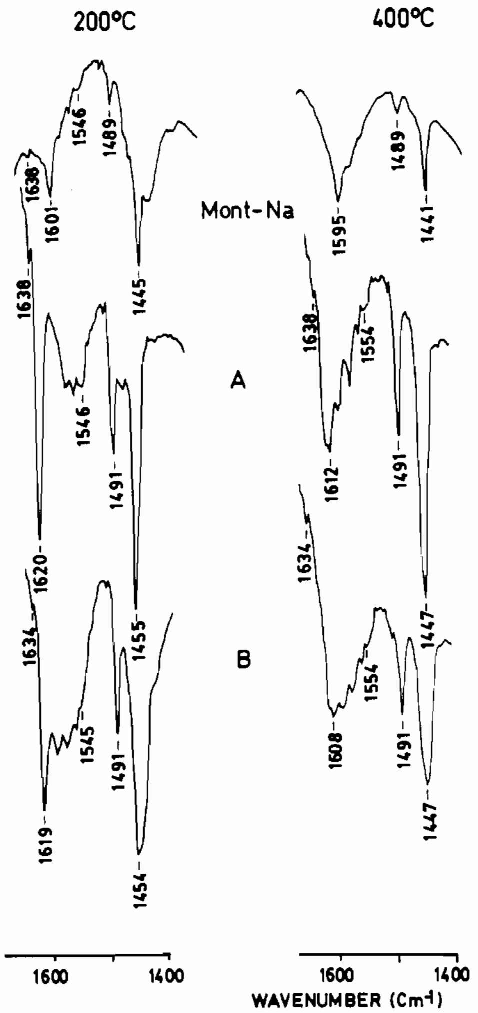

Figure 6. IR spectra of pyridine adsorbed on samples Mont-Na, A, and B.

Table IV. S_{BET} Expressed in Percent

sample	S_{BET}, % *a*	*b*	*c*
A	441	30	134
B	331	71	234
C	261	71	185
D	156	48	75
E	123	42	51

[a] Samples at room temperature with respect to sodium montmorillonite. [b] Samples treated at 700 °C with respect to the same untreated samples. [c] Samples treated at 700 °C with respect to Mont-Na.

morphology of natural montmorillonite. The increase in unpillared material as the percentage of Ga becomes greater is also confirmed by a peak in the thermograms at 600 °C together with a decrease in the water adsorbed on the surface as a consequence of the reduction in the surface area, seen in the zone of the DTG curves below 200 °C.

The N_2 adsorption data reflect great increases in the surface areas of samples A–C with respect to the original sample of Mont-Na (Table IV). The surface area of sample A, which is pillared only with Al, is 4.4 times that of the original sample, whereas the areas of samples B and C are respectively 3.3 and 2.6 times that of the original. The smaller increase in surface observed in samples B and C can be attributed to the lower percentage of pillared material.

However, it is more significant to observe the behavior of samples B and C under thermal treatment at 700 °C. While the surface area of sample A decreases to 115 m^2/g (30% of its untreated value and 134% of the value of Mont-Na), samples B and C retain surface areas that are still 71% of their untreated values (234 and 185%, respectively, of the value for Mont-Na). These data for the thermal stability of the surface area of the AlGa–PILCs (B and C) and Al–PILC (A) are in basic agreement with the results of Bardley and Kidd[13] although there are some minor differences between the two preparations, and in the case of Al–PILC we started with a material whose specific surface is considerably smaller (240 m^2/g). Furthermore, the volume of the micropores of sample A declines drastically after treatment at 700 °C (Table II) and there is an increase in the volume of its mesopores. Samples B and C, on the other hand, maintain a high percentage of microporosity and values of mesoporosity on the same order as in the untreated samples. Samples D and E present a much smaller increase in specific surface (Table IV) although it does appear that pillars are formed in a small fraction of the material (see X-ray diffractogram of Figure 1). Thermal treatment of these samples at 700 °C produces important reductions in their surface areas to values that are even smaller than that of the original montmorillonite. The authors cited above[13] obtained similar results for the stability of Ga–PILC although they started with a sample whose specific surface was greater (231 m^2/g). This suggests that the high content of Ga^{3+} is found not only in the form of pillars intercalated between the layers but also on the external surface, where, after thermal treatment, it blocks access of N_2 to the interlaminar spaces.

Even more striking are the results obtained after hydrothermal treatment. When the samples are heated to 500 °C under a current of humid air, it is found that the textural parameters of samples B and C remain basically the same as before treatment (Table III). By contrast, in sample A, pillared exclusively with Al, there is a total collapse of the pillars and the specific surface and microporosity fall sharply down to values similar to those of the initial sample of Mont-Na.

Analysis of the pyridine adsorption data indicates an increase in the acidity of the pillared samples with respect to the starting Mont-Na. Greater acidity is observed in sample A than in B, as a consequence of the fact that the quantity of Al^{3+} cation incorporated into sample A is greater than the amount of Al^{3+} + Ga^{3+} in the case of B. In both samples it is observed that the Lewis-type acidity is unaffected by thermal treatment whereas the Brönsted acid centers practically disappear at high temperatures, which indicates that the Lewis acid centers are stronger.

Conclusions

The material prepared with Al and Ga in certain proportions (samples B and C) is a product with stable mixed Al–Ga pillars (Al–Ga PILC). Its thermal and hydrothermal stability is greater than that of PILCs that are pillared only with Al, and at the same time, the new materials have similar acid properties. The thermal stability of samples B and C is indicated by the fact that after being treated at 700 °C for 2 h the specific surface conserves 71% of its value at room temperature. The sample treated hydrothermally at 500 °C retain 100% of their specific surface area. The high degree of stability of their textural properties together with the presence of acid centers on their surface make these materials potentially suitable for use in acid catalysis.

Acknowledgment. We acknowledge the Comisiön Investigaciön Cientifica y Tëcnica (CICYT) for financial support of this work under Projects MAT 88-0165 and L. Sanchez Aramburu by his collaboration in the SEM and EDXRA experiments.